2011

Thermoelectric Properties of ZnxInyOx+1.5y Films

Otto J. Gregory
University of Rhode Island

Matin Amani

Citation/Publisher Attribution
Gregory, Otto J. and Matin Amani. "Thermoelectric Properties of $Zn_xIn_yO_{x+1.5y}$ Films." Journal of the Electrochemical Society. 158(2):J15-J19. 2011.

Journal of The Electrochemical Society, **158** (2) J15-J19 (2011)
0013-4651/2010/158(2)/J15/5/$28.00 © The Electrochemical Society

Thermoelectric Properties of $Zn_xIn_yO_{x+1.5y}$ Films

Otto J. Gregory[z] **and Matin Amani**

Department of Chemical Engineering, University of Rhode Island, Kingston, Rhode Island 02881, USA

Ceramic thin film thermocouples are being developed to replace noble metal thermocouples operating within the harsh environments of advanced turbine engines used for power generation and propulsion. Seebeck coefficients as large as 158 μV/°C were determined for indium oxide (In_2O_3) at 950°C and 256 μV/°C for zinc oxide (ZnO) at 1250°C relative to platinum reference electrodes. Because these Seebeck coefficients are appreciably larger than those for metallic thermocouples, alloys in the system indium zinc oxide ($Zn_xIn_yO_{x+1.5y}$) were investigated by cosputtering from high purity ZnO and In_2O_3 targets. Thermocouple libraries were patterned with platinum reference electrodes and rapidly screened using combinatorial chemistry techniques. Thermoelectric response, power, and resistivity were determined for each thermocouple in the library. Thermocouples with the optimum compositions were prepared and the resulting power factor of the biceramic junctions was determined from 75 to 650°C.
 [DOI: 10.1149/1.3518412]

Manuscript submitted June 10, 2010; revised manuscript received October 25, 2010. Published December 8, 2010.

Thin film thermoelectric devices are being investigated for energy harvesting applications and temperature measurement in turbine engines used for propulsion and power generation. Thin film thermocouples[1] have a rapid response time (less than 1 μs) and can be directly deposited onto the surface of components without the need for adhesives or surface preparation.[2-6] Furthermore, thin films add negligible mass to the components and thus do not disturb the vibrational modes in smaller blades. They create minimal disturbance to the flow of gases over the surface,[7,8] because the thickness is well below the boundary layer thickness.

Thermoelectric devices are characterized by the dimensionless figure of merit, ZT, which is defined according to Eq. 1 as

$$ZT = S^2\sigma T/\kappa \quad [1]$$

where σ, κ, S, and T are the electrical conductivity, thermal conductivity, Seebeck coefficient, and absolute temperature, respectively. Because thermal conductivity measurements are difficult to make on thin films, the thermoelectric power factor according to Eq. 2 is normally defined as

$$\zeta = S^2\sigma = Z\kappa \quad [2]$$

In addition to a large Seebeck coefficient, thin film thermocouples require chemical and electrical stability; i.e., oxidation resistance as well as a stable Seebeck coefficient with little or no hysteresis. High electrical conductivity is not necessarily a requirement for measurement devices, but degradation of the electrical conductivity over time can result in output drift and device failure. Platinum–rhodium alloys have been used extensively for thin film thermocouple applications, but the signals can degrade at temperatures between 800 and 900°C due to oxidation and the films coalesce at elevated temperature leading to dewetting of the platinum films from oxide surfaces at elevated temperatures, which can lead to electromigration failures.[8] Selective rhodium oxidation can also result in inconsistent output due to thinning and poor adhesion.[2,5,8] In addition, the thermoelectric powers are relatively small and the catalytic nature of platinum can lead to significant errors (as much as 50°C) in the presence of certain hydrocarbons. Several attempts have been made to replace platinum based thermocouples but all have had poor performance or could not be used in oxidizing environments without employing protective coatings. For example, Bhatt et al. developed a $La_{(1-x)}Sr_xCoO_3$ and a TiC–TaC thin film thermocouple that yielded stable output at temperatures up to 1350 K.[4,7,9] However, the reported Seebeck coefficients of the thermocouples in these studies were quite small and their operational temperatures were relatively low compared to the temperatures typically encountered in the hot sections of turbine engines. Ohtaki et al.[10] systematically analyzed the thermoelectric properties of $Zn_{1-x-y}Al_xGa_yO$ produced by sintering ZnO, Al_2O_3, and Ga_2O_3 powders, in order to maximize ZT. Combinatorial studies using thin film libraries, which contain thermocouples with continuously varying compositions, have also been done using sputtering and pulsed laser deposition (PLD) to characterize the thermoelectric properties of $Zn_{1-x}Al_xO$, $(La_{1-x}Ca_x)VO_3$, and $(Ca_{1-x}B_x)_3Co_4O_9$ films.[11-16]

Wide bandgap, oxide semiconductors are ideal for both applications as they are already oxides and stable at high temperatures. Charge carriers in most transparent conducting oxides are usually attributed to oxygen vacancies according to Eq. 3

$$O_0^x \rightarrow 1/2O_2 + V_0^{\cdot\cdot} + 2e^{-1} \quad [3]$$

where $V_0^{\cdot\cdot}$ are doubly charged oxygen vacancies, as well as substitution of matrix cations with aliovalent impurities,[17] thus sputtering in partial pressures of oxygen decreases the electrical conductivity. $Zn_xIn_yO_{x+1.5y}$ has been investigated thoroughly as a transparent conducting oxide material through analysis of homologous compounds [$Zn_kIn_2O_{k+3}$, where k is an integer] and pseudobinary compounds produced by cosputtering.[18-20] Thermoelectric studies on bulk ZnO and In_2O_3 [$(ZnO)_mIn_2O_3$] ceramics have resulted in maximum ZT value at m = 3; however, the authors only investigated a few compositions.[21] In this paper we used cosputtering from multiple targets to form a high resolution (less than 2 wt % variation per thermocouple) concentration gradient of $Zn_xIn_yO_{x+1.5y}$ that depended on the relative distance from ZnO and In_2O_3 targets. Combinatorial chemistry techniques were used to rapidly screen the thermoelectric properties of the thermocouple libraries as a function of composition and heat-treatment.

Experimental Procedure

The $Zn_xIn_yO_{x+1.5y}$ films were deposited by radio-frequency (rf) sputtering using an MRC model 8667 sputtering system in which the rf power was evenly split between the two 15.2 cm diameter In_2O_3 and ZnO targets. Seven hundred and seventy (4.75 mm × 0.25 mm) thermoelements were prepared on a high purity (99.5%) alumina substrate using photolithography techniques to establish spatially dependent compositions. Prior to deposition, an aluminum oxide wafer was cleaned with methanol, acetone, and deionized water followed by a nitrogen blow dry. The thermocouple reference electrode and bond pads were patterned using a 50 μm thick dry film negative photoresist (MX5050, DuPont, Wilmington, DE) which can achieve a 75 μm linewidth and line spaces and has exceptional plasma resistance. The exposure was performed using a collimated UV light source (LS30, Optical Associates Inc., San Jose, CA) in conjunction with a contact photomask, and the thermocouple patterns were developed using a 1.5% DX-40 developer solution (RBP Chemical Technology, Milwaukee, WI). Platinum was deposited through the windows created in the resist to form bond pads and reference electrodes on the alumina substrate. Following deposition, the photoresist and excess film was lifted off in acetone. The lithog-

[z] E-mail: gregory@egr.uri.edu

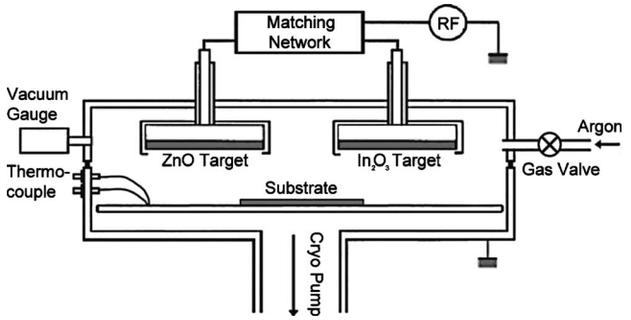

Figure 1. Schematic of an MRC 8667 sputtering system showing the positions of the two oxide sputtering targets relative to the work piece.

raphy processes was then repeated to pattern the $Zn_xIn_yO_{x+1.5y}$ thermocouple legs. Immediately following the semiconductor deposition, the entire process was repeated with an oxidized silicon wafer and the thicknesses of the deposited films on the silicon wafer were determined using a Sloan Technology Corporation, Goleta, CA DEKTAK II surface profilometer, to determine the resistivity of the films.

The platinum bond pads and reference electrodes were sputtered from a high purity (99.99%) 100 mm diameter platinum target at an rf power of 300 W and an argon pressure of 1.87 Pa, resulting in a 3 μm thick film. The cosputtered $Zn_xIn_yO_{x+1.5y}$ films were fabricated by placing the alumina substrate between simultaneously energized In_2O_3 and ZnO targets (Fig. 1) in 1.33 Pa argon pressure. Because relatively thick films are required for thermoelectric device applications, the oxide semiconductor films were deposited at 400 W for 30 h. This produced a nominal film thickness of 1.8 μm. The sputtering voltage was divided evenly between the two targets and the tuning parameters were maintained throughout the sputtering run to preserve a uniform composition gradient, producing compositions ranging from $\delta = 0.05$ to 0.92 where the ratio δ is defined as $W_{In}/(W_{In} + W_{Zn})$, where W_{In} and W_{Zn} are the mass percentages of indium and zinc. Prior to sputtering, a background pressure of less than 1.13×10^{-4} Pa was achieved in the vacuum chamber. The targets were presputtered onto shutters for 30 min in order to release trapped water vapor and remove cross contaminants derived from other targets. The wafer temperature was held at 25°C by water cooling during sputtering; because the rf power is split between two targets, there is negligible heating of the substrate throughout the deposition.

After deposition, the thin film thermocouples were heat-treated for 5 h at 500°C in a high purity nitrogen atmosphere and tested for thermoelectric output. The samples were retested after annealing in air at 500°C for 1 h. The thermocouples were tested by recording the voltage drop across the device with a USB Data Acquisition system (IOtech Personal Daq 54, Measurement Computing Corporation, Norton, MA) using Personal DaqView software, while applying a constant temperature gradient of 7.7 K with a hot probe. In order to determine the Seebeck coefficients, the surface temperatures of the hot and cold junctions were verified using thin film type-K thermocouples sputtered directly on the alumina wafer. The resistivities of the films were determined by measuring the resistance and thickness of each leg after deposition and each heat-treatment step. Micrographs of the cosputtered ceramic films were obtained using a JEOL 5900 scanning electron microscope (SEM). Compositions of the films were also determined using the SEM with energy-dispersive X-ray spectroscopy (EDS). For the two most promising materials the oxygen content was determined using Auger electron spectroscopy (AES) with a Perkin-Elmer 5500 multitechnique surface analyzer; the surfaces were sputter etched for 12 s in order to remove surface contaminants from the sample. To determine the Seebeck coefficients, the thermoelectric response was fit to

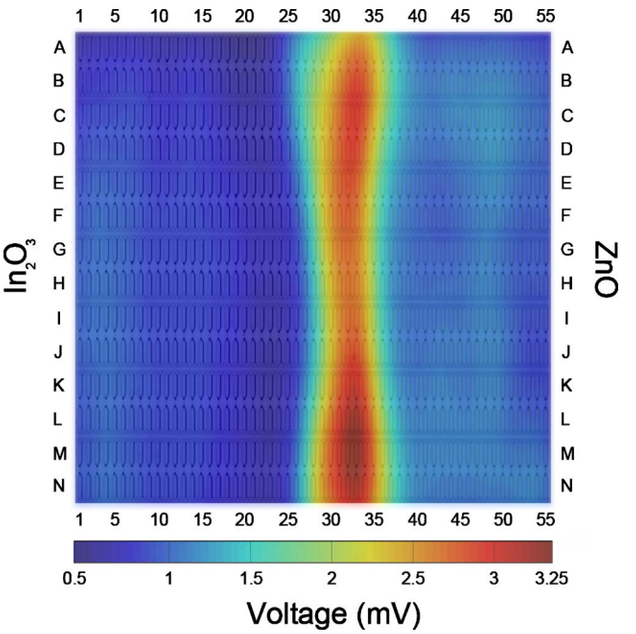

Figure 2. (Color online) Map showing the thermoelectric response of the nitrogen annealed $Zn_xIn_yO_{x+1.5y}$ library when a temperature gradient of $\Delta T = 7.7$ K was applied.

a second-order autoregressive process using the least-squares method and the equilibrium output voltages were determined. EDS was used after deposition to determine the compositions of 50 thermocouples in the library.

Four thermocouples having an optimal $Zn_xIn_yO_{x+1.5y}$ composition for both thermoelectric power and Seebeck coefficient were sputtered on 130 mm × 25 mm alumina substrates and annealed at 500°C for 5 h in nitrogen, followed by an anneal at 800°C for 1 h in air. The alumina substrate was placed into the hot zone of a tube furnace (MHI H18-40HT, Micropyretics Heaters International Inc., Cincinnati, OH) where a temperature gradient was applied along the length of the substrate, by placing a heat shield in the middle of the rectangular substrate. The cold junction was maintained at 20°C using an ethylene glycol coolant circulated through a Thermo Neslab Inc., Newington, NH NESLAB chiller that was connected to an aluminum chill block. The furnace was thermally cycled from room temperature to 800°C at a heating/cooling rate of 3°C/min in air. In order to determine the thermoelectric power factor for the material, resistivity and the temperature coefficient of resistivity as well as any hysteresis in the resistivity of the sputtered film were also determined using the Van der Pauw method.

Results and Discussion

The thermoelectric responses of the thin film thermocouple libraries are shown in Fig. 2 and 3, where a temperature gradient of 7.7 K was applied. A polynomial surface was fit to the data, allowing the thermocouples to be sorted by composition according to the thermoelectric maps obtained from the raw library data shown in Fig. 2 and 3. Ultimately two-dimensional plots were created from the surface maps to show the thermoelectric properties as a function of indium content (Fig. 4 and 5).

Figure 4 shows the dependence of the electrical conductivity of the films as a function of δ in the resulting thermocouple libraries, which is consistent with the results observed by Moriga et al.[19] for room temperature combinatorial depositions of In_2O_3 and ZnO. Seebeck instability prior to heat-treatment in air was previously studied in indium tin oxide thin film thermocouples used at temperatures higher than 600°C.[22-26] Compensation of the oxygen vacancies at high temperature during prolonged exposure in air reduces the car-

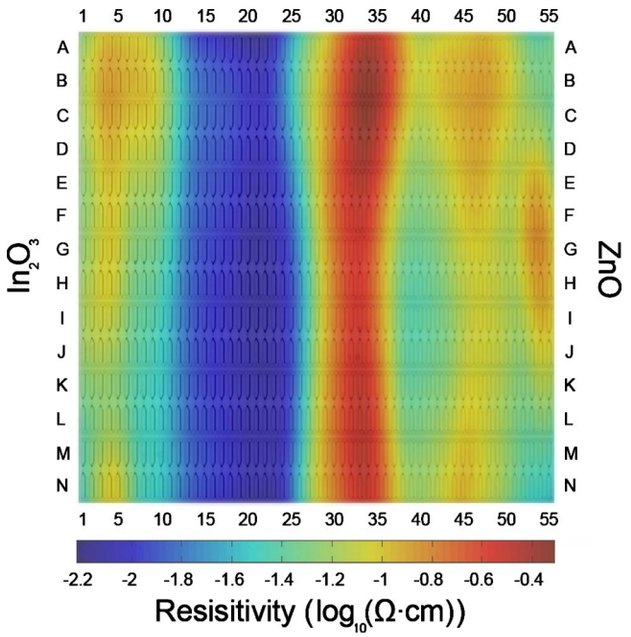

Figure 3. (Color online) Map showing the resistivity of the nitrogen annealed $Zn_xIn_yO_{x+1.5y}$ library at room temperature.

rier concentration. As a result the hysteresis of the electrical conductivity shows that prior to exposure at high temperatures these materials behave like degenerate semiconductors because the electrical conductivity is inversely proportional to temperature. In most applications, the films comprising the cold junction are never exposed to peak operating temperature, which results in variation of the carrier concentration along the length of the device. Inhomogeneities in the films comprising the hot and cold junctions can lead to noise, drift, and voltage spikes in the thermoelectric response. Several attempts have been made to eliminate these spikes including deposition of thicker films and use of alumina protective overcoats; however, additional heat-treatments in air have produced the most promising results to date.[22] These heat-treatments were also performed on the thermoelectric libraries to fully characterize the behavior and stability of the materials. Further instability can also be caused by sublimation and decompositions of films in oxygen deficient atmospheres. Once the films have been heat-treated in air to stabilize the carrier concentration, plasma sprayed $MgAl_2O_4$ coatings and alumina pastes have been successfully used to reduce sublimation effects in transparent conducting oxides.

An initial heat-treatment in nitrogen at 500°C for 5 h was performed to help increase density of the films, reduce defects, alleviate blistering of films caused by coalescence of trapped argon, and improve the grain size. A rapid decrease in the conductivity was observed in the same range of compositions that produced a peak in Seebeck as shown in Fig. 5a. After further heat-treatment in air at 500°C for 1 h, the conductivity of these films was further reduced. The Seebeck coefficient also increased dramatically as shown in Fig.

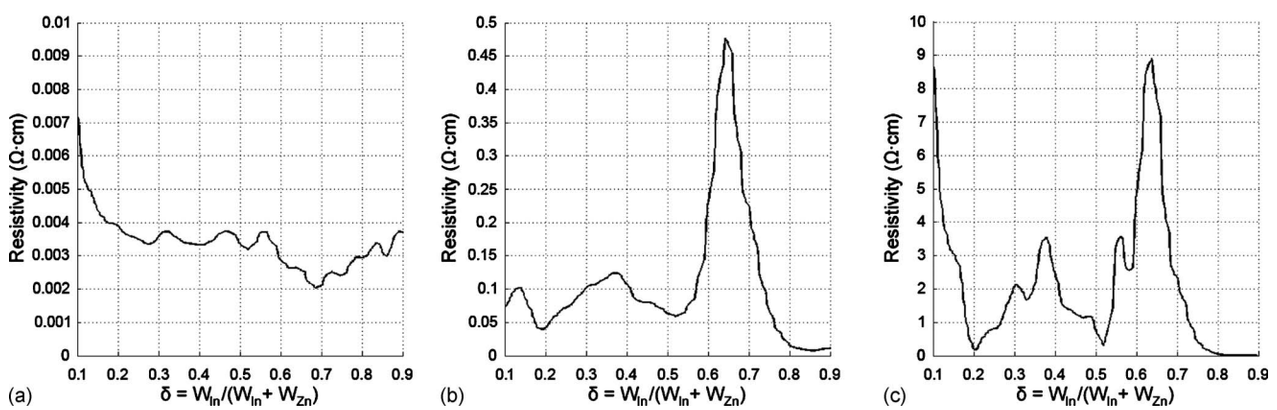

Figure 4. Effect of indium content on the electrical resistivity of (a) as deposited, (b) nitrogen annealed, and (c) air annealed thin films.

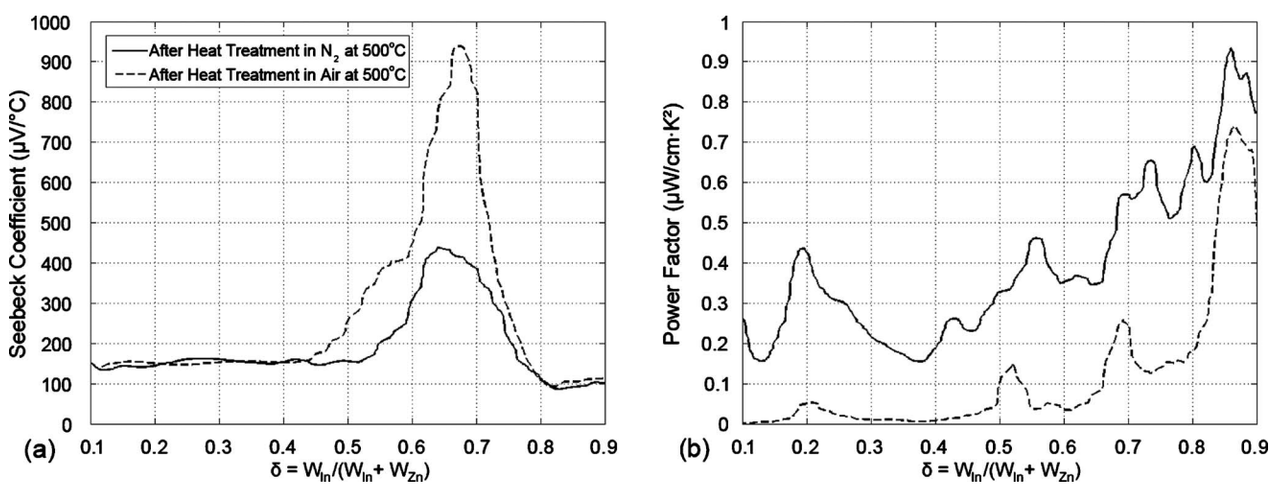

Figure 5. Effect of indium content on (a) the Seebeck coefficient, and (b) the power factor after various heat-treatments.

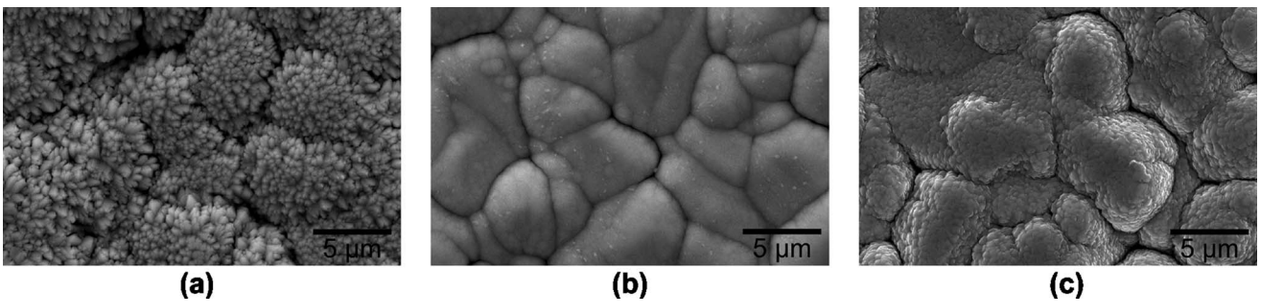

Figure 6. SEM micrographs of cosputtered (a) In_2O_3 ($\delta = 0.97$), (b) $Zn_2In_6O_{11}$ ($\delta = 0.85$), and (c) ZnO ($\delta = 0.04$) thermocouples taken after annealing in N_2 for 5 h at 500°C.

5a, suggesting that compensation of the oxygen vacancies selectively increased phonon scattering in the zinc rich thermocouples ($\delta = 0.1$ to 0.55). These show no improvement in Seebeck but resulted in a marked decrease in conductivity, which significantly reduced the power factor, as depicted in Fig. 5b. The thermocouples with the largest and most stable power factor were in the range of $\delta = 0.85$ to 0.95. These showed only a slight decrease in the electrical conductivity and no change in the Seebeck after heat-treatment. It should also be noted that the films exhibited a negative Seebeck coefficient and n-type behavior. SEM micrographs of the films show that the evolution of the grain structure and morphology was observed as a function of position/composition of the thermocouples (Fig. 6). A microstructure typical of cosputtered films[19] was observed for zinc rich compositions ($\delta < 0.92$) and indium oxide rich compositions ($\delta > 0.11$). The indium oxide rich thermocouples shown in Fig. 6a indicate submicrometer grains with a platelike habit or morphology and the grains within a given cluster are randomly oriented. Because the devices were patterned in photoresist using photolithography processes, the substrate was maintained at a relatively low temperature, for which cosputtered films of these materials have been shown to result in poor crystallinity and thus are typically amorphous.[19] This was observed in Fig. 6b, where no fine structure or platelike morphology was observed in the microstructures shown in Fig. 6a and 6c.

The Seebeck coefficient, resistivity, and power factor were established for the two most promising compositions; i.e., $\delta = 0.85$ corresponding to $Zn_2In_6O_{11}$ having the largest power factor and $\delta = 0.72$ corresponding to $Zn_4In_6O_{13}$ having the largest Seebeck coefficient. The stoichiometry of the film was confirmed using AES, which can provide a quantitative estimate of the oxygen content of the film while EDS can only determine the ratio of indium to zinc. The absolute Seebeck of these optimal compositions was determined by subtracting the absolute Seebeck coefficient of platinum, which was determined by interpolating data from Moore et al.[27] using the least-squares fit to a fourth-order polynomial shown in Eq. 4

$$S_{Pt} = (1.452 \times 10^{-11})T^4 - (5.958 \times 10^{-8})T^3 + (8.717 \times 10^{-5})T^2 - 0.0687T + 9.23 \quad [4]$$

Our data also shows that ZnO thermocouples, as well as the cosputtered thermocouples shown in Fig. 7b and 8, experienced a change in slope of the Seebeck around 575°C, which was also observed for bulk ZnO based ceramics prepared by Ohtaki et al. and Tanaka et al.[10,28] While the library results show that at room temperature all of the thermoelements are n-type, the derivative of the Seebeck curve for $Zn_4In_6O_{13}$ shows a change in sign at 280 and 560°C, which suggests that p-type charge carriers are being generated but not in sufficient concentrations to make the Seebeck positive. A similar effect has been observed in ITO strain gauges at high temperatures, where tin donors dominate the doubly charged oxygen vacancies at temperatures above 950°C. Despite the fact that both In_2O_3 and SnO_2 are n-type semiconductors from room temperature to 1500°C, the piezoresistive response changes sign at 950°C.[29] Because the cold junction is maintained at room temperature during the test, it cannot be determined if the material changes type at high temperatures. This measurement can be done by applying a differential tem-

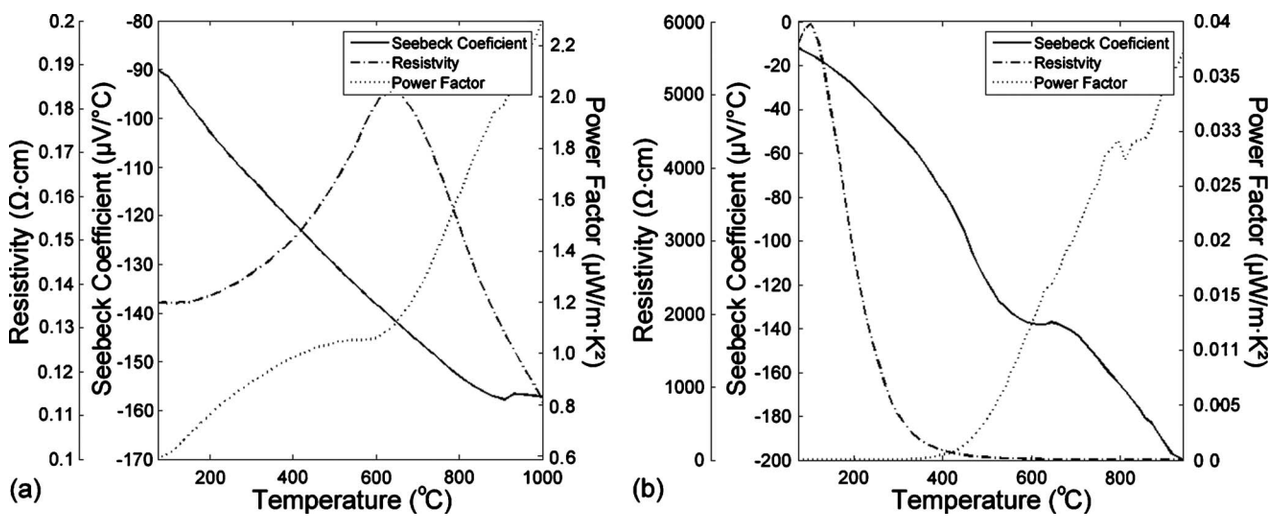

Figure 7. Absolute Seebeck, electrical resistivity, and power factor of pure (a) In_2O_3 and (b) ZnO films after annealing at 500°C in N_2 for 5 h and 1000°C in air for 1 h.

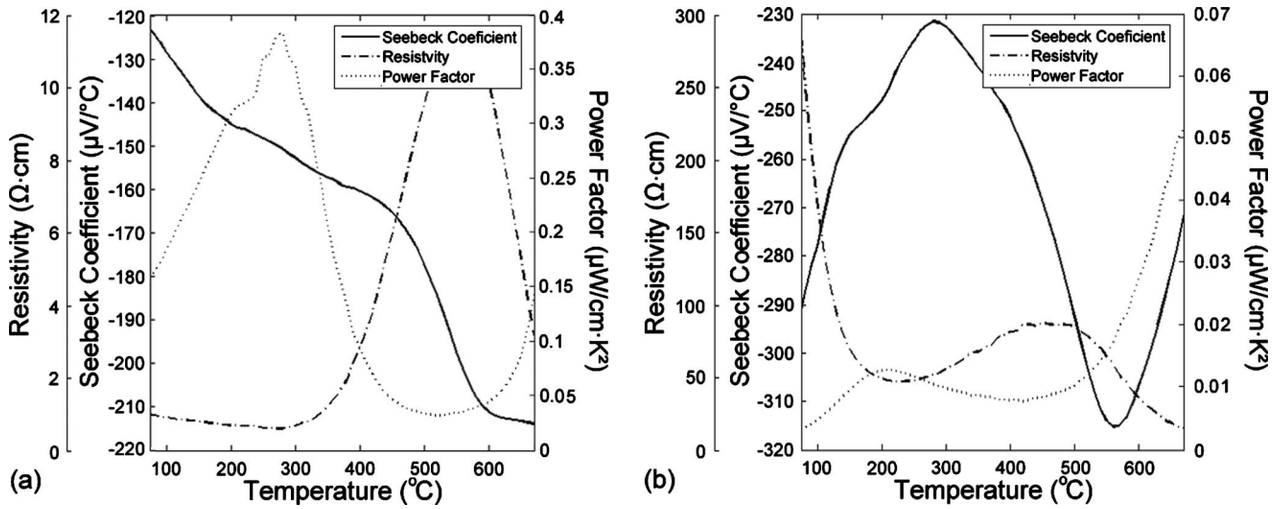

Figure 8. Absolute Seebeck, electrical resistivity, and power factor of (a) $Zn_2In_6O_{11}$ and (b) $Zn_4In_6O_{13}$ films after annealing at 500°C in N_2 for 5 h and 1000°C in air for 1 h.

perature gradient in varying background temperatures and will be further investigated. Work on bulk ceramics has been done in this system focusing on the zinc rich end of the spectrum, thereby producing the compound $(ZnO)_3In_2O_3$ (corresponding to $\delta = 0.54$) as the composition having the maximum ZT.[21] This composition resulted in a local maximum in the power factor in the system In_2O_3–ZnO.

Conclusion

A wide range of compositions in the system $Zn_xIn_yO_{x+1.5y}$ were investigated for their thermoelectric response. They were successfully characterized in terms of Seebeck coefficient, electrical conductivity, and power factor. The thin film thermocouples with the two most promising compositions were then fabricated and tested at significantly higher temperatures, which showed much higher Seebeck coefficients than either of the ZnO or In_2O_3 end members. The results from the two most promising compositions confirmed those results obtained from the combinatorial library. Studies based on the screening experiments are currently being performed using plasma sprayed sputtering targets and bulk ceramics of the two most promising compositions. Moreover, the Seebeck data suggest that p-type charge carriers are present in $Zn_4In_6O_{13}$ at higher temperatures, indicating that a p-type thermoelectric material may be developed for high temperature applications.

Acknowledgments

The authors thank the NASA Glen Research Center, Cleveland, OH for the support of this work under NASA Grant NNX07AB83A (Aircraft Ageing and Durability Project). We acknowledge the help of Ian Tougas of the Department of Chemical Engineering at the University of Rhode Island for completing the thickness measurements, and Michael Platek of the Electrical Engineering Department at the University of Rhode Island for help with AES and SEM.

University of Rhode Island assisted in meeting the publication costs of this article.

References

1. H. Choi and X. Li, *Sens. Actuators, A*, **136**, 118 (2007).
2. J. F. Lei and H. A. Will, *Sens. Actuators, A*, **65**, 187 (1998).
3. L. C. Martin and R. Holanda, *NASA Tech. Memo.*, TM-106714 (1994).
4. H. D. Bhatt, R. Vedula, S. B. Desu, and G. C. Fralick, *Thin Solid Films*, **342**, 214 (1999).
5. K. G. Kreider, *J. Vac. Sci. Technol. A*, **11**, 1401 (1993).
6. K. G. Kreider and M. Yust, U.S. Pat. 4,969,956 (1990).
7. R. Holanda, *NASA Tech. Memo.*, **TM-106017**, 649 (1992).
8. G. E. Aniolek and O. J. Gregory, *Surf. Coat. Technol.*, **68–69**, 70 (1994).
9. H. D. Bhatt, R. Vedula, S. B. Desu, and G. C. Fralick, *Thin Solid Films*, **350**, 249 (1999).
10. M. Ohtaki, K. Araki, and K. Yamamoto, *J. Electron. Mater.*, **38**, 1234 (2009).
11. J. D. Wrbanek, G. C. Fralick, S. C. Farmer, A. Sayir, C. A. Blaha, and J. M. Gonzalez, *NASA Tech. Memo.*, TM-213211 (2004).
12. R. Funahashi, S. Urata, and M. Kitawaki, *Appl. Surf. Sci.*, **223**, 44 (2004).
13. K. C. Hewitt, P. A. Casey, R. J. Sanderson, M. A. White, and R. Sun, *Rev. Sci. Instrum.*, **76**, 093906 (2005).
14. H. Minami, K. Itaka, H. Kawaji, Q. J. Wang, H. Koinuma, and M. Lippmaa, *Appl. Surf. Sci.*, **197–198**, 442 (2002).
15. K. Itaka, Q. J. Wang, H. Minami, H. Kawaji, and H. Koinuma, *Appl. Surf. Sci.*, **223**, 20 (2004).
16. M. Otani, N. D. Lowhorn, P. K. Schenck, W. Wong-Ng, M. L. Green, K. Itaka, and H. Koinuma, *Appl. Phys. Lett.*, **91**, 132102 (2007).
17. S. P. Harvey, T. O. Mason, D. B. Buchholz, R. P. H. Chang, C. Körber, and A. Klein, *J. Am. Ceram. Soc.*, **91**, 467 (2008).
18. T. Moriga, D. D. Edwards, T. O. Mason, G. B. Palmer, K. R. Poeppelmeier, J. L. Schindler, and C. R. Kannewurf, *J. Am. Ceram. Soc.*, **81**, 1310 (1998).
19. T. Moriga, T. Okamoto, K. Hiruta, A. Fujiwara, I. Nakabayashi, and K. Tominaga, *J. Solid State Chem.*, **155**, 312 (2000).
20. H. Hiramatsu, W. S. Seo, and K. Koumoto, *Chem. Mater.*, **10**, 3033 (1998).
21. H. Kaga, R. Asahi, and T. Tani, *Jpn. J. Appl. Phys.*, **43**, 3540 (2004).
22. X. Chen, O. J. Gregory, and M. Amani, *J. Am. Ceram. Soc.*, In press.
23. O. J. Gregory, E. Busch, G. C. Fralick, and X. Chen, *Thin Solid Films*, **518**, 6093 (2010).
24. O. J. Gregory, Q. Luo, and E. E. Crisman, *Thin Solid Films*, **406**, 286 (2002).
25. K. G. Kreider and G. Gillen, *Thin Solid Films*, **376**, 32 (2000).
26. K. G. Kreider, *Sens. Actuators, A*, **34**, 95 (1992).
27. J. P. Moore and R. S. Graves, *J. Appl. Phys.*, **44**, 1174 (1973).
28. Y. Tanaka, T. Ifuku, K. Tsuchida, and A. Kato, *J. Mater. Sci. Lett.*, **16**, 155 (1997).
29. O. J. Gregory, Q. Luo, J. M. Bienkiewicz, B. M. Erwin, and E. E. Crisman, *Thin Solid Films*, **405**, 263 (2002).